ACUSTICA · acta acustica
Vol. 83 (1997) 297 – 303

Accurate Power Spectrum Estimation of a Damped Sinusoidal Signal in Low SNR Cases Based on a Newly Defined Transfer Function

Hiroshi Kanai, Masaki Imai, and Noriyoshi Chubachi
Department of Electrical Engineering, Faculty of Engineering, Tohoku University, Aramaki-aza-Aoba, Sendai 980, Japan

Summary
This paper is concerned with a method to estimate the power spectrum of a periodic damped sinusoidal signal contaminated by high-level noise components when there are fluctuations in the period. A correlation between two spectral components exists at and around the resonant frequency of a damped sinusoidal signal. By using this property, the authors introduce a new transfer function defined from the resonant frequency component to every other component around the resonant frequency to estimate the power spectrum of the damped sinusoidal signal. Since it can be assumed that there is no correlation between these two different frequencies for the noise components, the noise components in the cross spectrum at the two different frequencies decrease with the averaging operation. Consequently, the power spectrum of the damped sinusoidal signal is accurately estimated from the observed signals, even if the signal-to-noise ratio (SNR) is very low. The proposed method developed here is satisfactorily confirmed by simulation experiments. This method is further applied to the estimation of the power spectra of the vibration signals radiated from normal and defective automobile engines.

PACS no. 43.35.Bf

1. Introduction

Resonant vibration induced by a defect in a mechanical system such as an automobile engine is modelled by the following damped sinusoidal wave, $x(n)$:

$$x(n) = \mathrm{e}^{-\alpha n T_S} \cos(\omega_0 n T_S), \quad (n = 0, 1, ...) \qquad (1)$$

where T_S is the sampling period, α is the damping factor, and ω_0 is the resonant angular frequency of the resultant vibration as shown in Figures 1(a) and 1(b).

In a defective automobile system, the defect-induced signal $x(n)$ is almost always periodically generated with an interval $T_0 = N_0 T_S$ as shown in Figure 1(d). Thus, the resultant observed signal $y(n)$ is described by the sum of the iteratively generated signal $x(n)$ and an additive noise signal $w(n)$ as follows:

$$y(n) = x(n) * \sum_m \delta(n - mN_0 - \tau_m) + w(n), \qquad (2)$$

where $*$ denotes a convolution, m is an integer describing the ignition number, $\delta(n)$ is the impulse due to the ignition, $\tau_m \times T_S$ is the time delay associated with the mth impulse $\delta(n - mN_0)$ in Figure 1(c), that is, the period from the mth ignition timing of Figure 1(c) to the defect-induced-vibration being radiated during each explosion period in Figure 1(d), and $w(n)$ is the noise component which is caused even when the automobile system is normal. In this paper, $w(n)$ is assumed to be Gaussian white noise, which is uncorrelated with $x(n)$, and the repetition interval $T_0 = N_0 \times T_S$ is much longer than the duration period of the damped sinusoidal signal $x(n)$ as shown in Figure 1(d). Though the impulse train due to ignition pulses is given by $\sum_m \delta(n - mN_0)$, which is just periodic as shown in Figure 1(c), the term $\sum_m \delta(n - mN_0 - \tau_m)$ in equation (2) shows the impulse train, the repetition interval of which is almost T_0 due to the ignition signal but which contains fluctuations.

Received 23 February 1993, to be published in ACUSTICA, accepted 20 December 1995.

Let us re-define the resonant vibration signal $x(n;m)$ and noise signal $w(n;m)$, respectively, in the mth block just after the mth ignition timing by

$$\begin{aligned} x(n;m) &= x(n + mN_0) \\ &= x(n) * \delta(n - \tau_m) \quad (n = 0, ..., N_0), \qquad (3) \\ w(n;m) &= w(n + mN_0) \qquad (n = 0, ..., N_0). \qquad (4) \end{aligned}$$

The observed signal $y(n;m)$ in the mth block is given by

$$y(n;m) = x(n;m) + w(n;m) \quad (n = 0, ..., N_0). \qquad (5)$$

There are two standard methods to estimate the resonant vibration component $x(n)$ or its power spectrum $|X(k)|^2$ from the observed signal $y(n)$ by reducing the noise component $w(n)$: first, by averaging operation in the time domain, the observed signal $y(n)$ is divided into block signals $\{y(n;m)\}$ in equation (5) by referring to the ignition timing, which is completely periodic, and then the resultant periodic signals $\{y(n;m)\}$ are summed up at the same timing. The resultant averaged signal is given by

$$\begin{aligned} E[y(n;m)] &= E[x(n;m)] + E[w(n;m)] \\ &= x(n) * E[\delta(n - \tau_m)] + E[w(n;m)], \quad (6) \end{aligned}$$

where $E[\cdot]$ represents the average operation. If the noise component $w(n;m)$ in the mth block is uncorrelated with $w(n;l)$ in the lth block ($l \neq m$), the noise component of the second term in equation (6) decreases in proportion to $1/\sqrt{M}$, where M is the number of samples averaged. That is, the averaging operation in the time domain is effective in reducing the noise component $w(n)$ when the term τ_m is kept unchanged. In actual automobile systems, however,

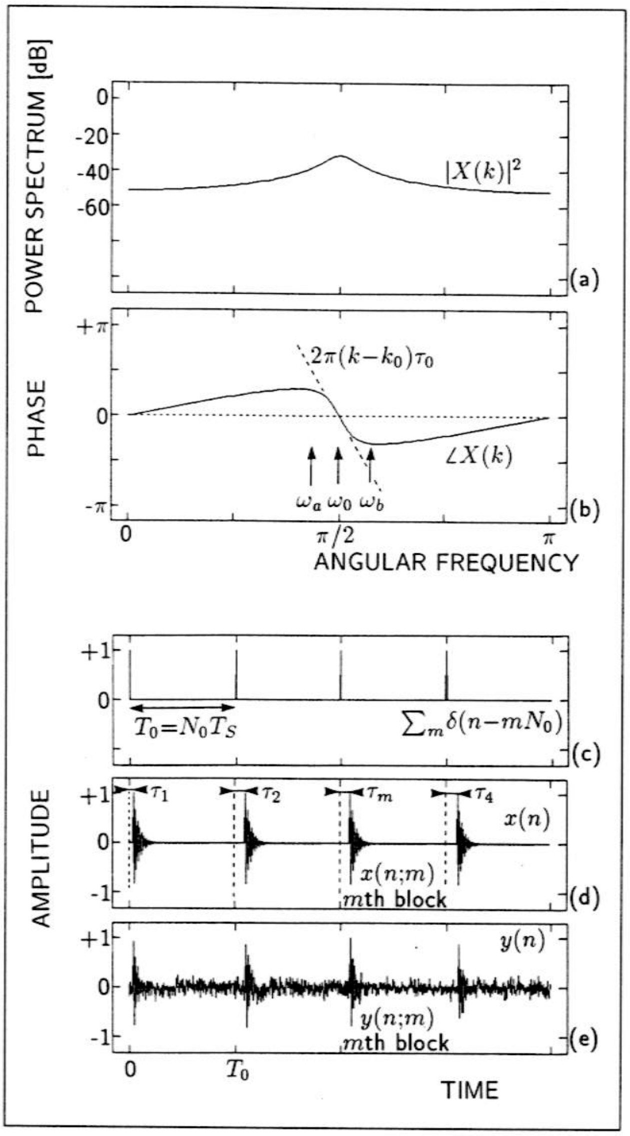

Figure 1. The aperiodic damped sinusoidal signal $x(n)$ and the model of the measured signal $y(n)$.
(a) The power spectrum $|X(k)|^2$ of the resonant vibration $x(n)$.
(b) The phase characteristic $\angle X(k)$ of $x(n)$.
(c) The periodic impulse train $\sum_m \delta(n - mN_0)$.
(d) The aperiodic damped sinusoidal signal $x(n) * \sum_m \delta(n - mN_0 - \tau_m)$, which can be divided into block signals.
(e) The model of the measured signal $y(n)$, (S/N=-5.0 dB), which is also divided into block signals $y(n;m)$.

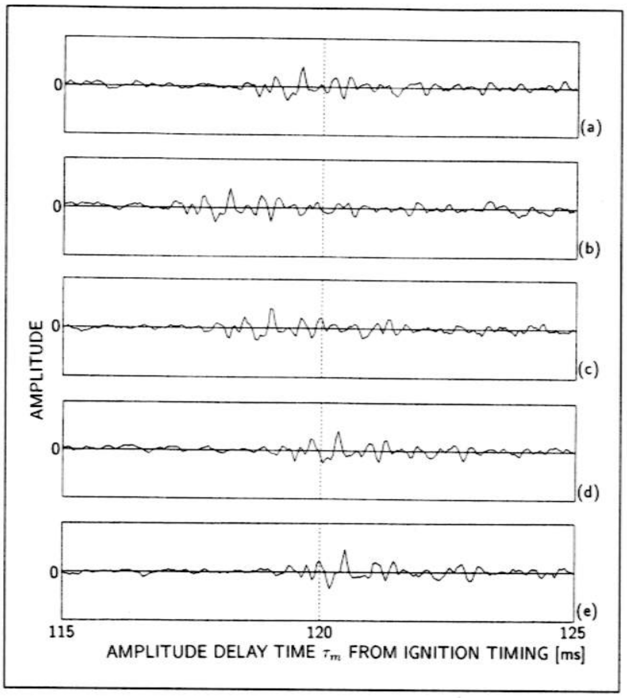

Figure 2. An example of the defect-induced signals being generated with fluctuations in the time domain, as is the case in an actual automobile system. (a)-(e) show the vibrations in the period around τ_m from each ignition timing for five succeeding explosion periods.

there are large fluctuations in the measured values $\{\tau_m\}$ of the lag term as shown in Figure 2. When the SNR is low, it is difficult to detect accurately the start of each timing, $\tau_m + mN_0$, of the defect-induced signal $x(n;m)$ in the mth block from the observed noisy signal $y(n;m)$. Thus, in using the average operation in the time domain, the resonant vibration component to be estimated in the first term of equation (6) also decreases in proportion to $1/\sqrt{M}$. Therefore, this method cannot be applied to an automobile system to estimate the resonant vibration signal.

Secondly, in the standard fast Fourier transform (FFT)-based method [1], $y(n)$ is also divided into block signals $y(n;m)$ in equation (5), and then the power spectra $|Y(k;m)|^2$ of $y(n;m)$ are averaged. Since the effect due to the fluctuation in the lag values $\{\tau_m\}$ is almost negligible in each power spectrum $|Y(k;m)|^2$, the resultant averaged power spectrum $P_y(k)$ of $y(n)$ is given by

$$\begin{aligned} P_y(k) &= E\big[|Y(k;m)|^2\big] \\ &= E\big[|X(k;m)|^2\big] + E\big[|W(k;m)|^2\big] \\ &= |X(k)|^2 + E\big[|W(k;m)|^2\big], \end{aligned} \tag{7}$$

where $X(k)$, $X(k;m)$, and $W(k;m)$ are the spectra obtained by applying the N_0-point FFT to the signals $x(n)$, $x(n;m)$, and $w(n;m)$, respectively. However, the noise component $E\big[|W(k;m)|^2\big]$ cannot be reduced even though the average number M of equation (7) is increased to infinity. Thus, the resultant power spectrum which estimates $P_y(k)$ includes a significantly large noise component, especially when the SNR is low.

For the problem of reducing the noise component in the observed *aperiodic* signal, therefore, using time-domain averaging, both the noise component and the signal component decrease. Using power spectrum averaging, the fluctuations in the phase of the signal become unimportant but the noise component cannot be reduced.

There is correlation between two frequency components at and around the resonant frequency of the damped sinusoidal signal $x(n)$. In order to detect the correlation between these two different frequency components of $x(n)$, the newly-defined squared coherence function between these two different frequency components is proposed in [2]. Using this coherence function, it is confirmed that there is correlation between two different frequency components of the resonant vibration by experiments. By utilizing the existance of a correlation between different frequency components of the resonant vibration $x(n)$, we define a new transfer function from the spectrum component at the resonant frequency to those around the resonant frequency. Using this transfer function, we propose a new method accurately to estimate the power spectrum $|X(k)|^2$ of $x(n)$ in equation (2) from the observed signal $y(n)$ even when the SNR is very low. By this method, the power spectrum of the noise component is decreased in proportion to $1/\sqrt{M}$, which cannot be achieved by the standard FFT-based method of equation (7).

2. Principle

As is shown in the spectrum $X(k)$ of the resonant vibration $x(n)$ in Figures 1(a) and 1(b), there is a correlation between two different angular frequency components at ω_a and ω_b near the resonant angular frequency ω_0 of $x(n)$. That is, the relation between the spectral components $X(\omega_a; m)$ and $X(\omega_b; m)$ of the mth block signal $x(n; m)$ is always kept constant for every block, even if there are fluctuations in the lag values $\{\tau_m\}$. Thus, this paper newly introduces a transfer function $H_{ab}(k)$ from one frequency component $X(\omega_a)$ at ω_a to another $X(\omega_b)$ at ω_b in the signal $x(n)$. From this transfer function, the complex ratio of $X(\omega_b)$ to $X(\omega_a)$ is determined. By averaging the transfer function, the power spectrum $|X(k)|^2$ of the damped sinusoidal signal $x(n)$ is estimated even when it is contaminated by high-level noise components $w(n)$ because the complex ratio of the spectra $W(\omega_b)$ at ω_b to $W(\omega_a)$ at ω_a for the noise components varies randomly. In order to obtain the transfer function $H_{ab}(k)$ defined between these different frequency components ω_a and ω_b, ($\omega_a \neq \omega_b$), both the $X(\omega_a)$ and $X(\omega_b)$ components should be transformed in the first step of the proposed procedure so that they share the same frequency band as described below.

Let $y_i(n; m)$, $(i = a, b, ...)$ be the signal in the mth block of the narrow-band signal which is obtained by applying the band-pass-filter, whose discrete central frequency is k_i and whose discrete frequency band is $[k_i - \Delta k, k_i + \Delta k]$ as shown in Figure 3(a-1), to the observed signal $y(n)$. The two different narrow-band signals $y_a(n; m)$ and $y_b(n; m)$ do not share the same frequency band at this stage if $a \neq b$. Thus, by the standard transfer function, the ratio of the spectrum $Y_b(k; m)$ of $y_b(n; m)$ to the spectrum $Y_a(k; m)$ of $y_a(n; m)$ is not determined. Using the square operation for each narrow-band signal $y_i(n; m)$, $(i = a, b)$ in the time domain, the resultant squared signal $z_i(n; m) = |y_i(n; m)|^2$ has the same frequency band around the d.c. component as shown in Figures 3(b-1) and 3(b-2). These derivations are described as follows: Since the squaring operation in the time domain coincides with the convolution in the frequency domain [4, p. 95], the spectrum $Z_i(k; m)$ of the squared signal $z_i(n; m)$ of $y_i(n; m)$ in the mth block is given by

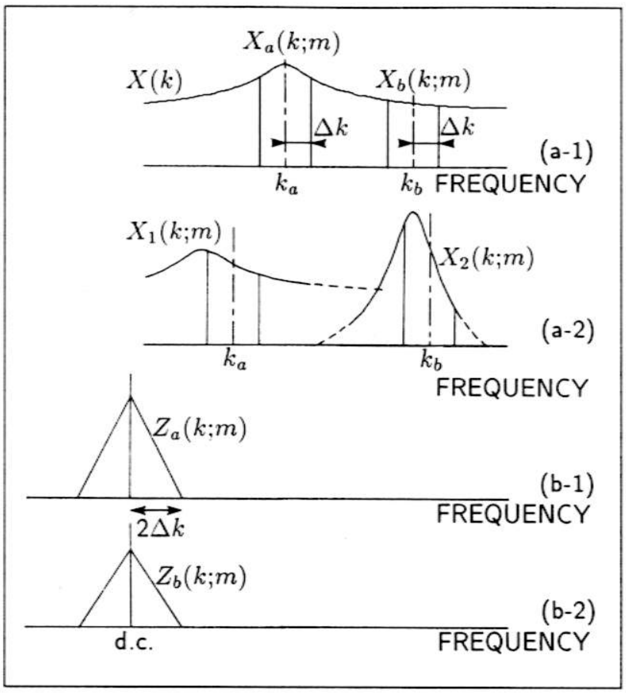

Figure 3. An illustration explaining the principle of the proposed method.

$$Z_i(k; m) = \frac{1}{N_0} \sum_{l=0}^{N-1} Y_i(l; m) Y_i^*(l - k; m) = \frac{1}{N_0} \sum_{l=k_i-\Delta k}^{k_i+\Delta k} Y_i(l; m) Y_i^*(l - k; m), \qquad (8)$$

where $i = a, b$ and * denotes the complex conjugate, and N_0 is the number of points in the FFT. Thus, as shown in Figures 3(b-1) and 3(b-2), the spectra $Z_a(k; m)$ of $z_a(n; m)$ and $Z_b(k; m)$ of $z_b(n; m)$ have components in the same low frequency band around the d.c. component no matter what discrete frequency band $[k_i - \Delta k, k_i + \Delta k]$ the original narrow-band signal $y_i(n; m)$, $(i = a, b)$, has.

Next, let us consider the physical meaning of the spectrum $Z_i(k; m)$ of the squared signal $z_i(n; m) = |y_i(n; m)|^2$ in equation (8). As shown in the spectrum $X(k)$ of the resonant vibration $x(n)$ of Figures 1(a) and 1(b), when the duration time of the defect-induced vibration $x(n)$ is very short, the spectrum $X(k)$ of $x(n)$ has an almost constant magnitude, $|X(k_i)|$, and smooth phase characteristics of $\theta(k) = 2\pi(k - k_0)\tau_0$ around the resonant angular frequency ω_0, where $k_0 = N_0\omega_0/2\pi$ denotes the discrete centre frequency of the resonant vibration and τ_0 is the gradient of the phase around k_0. Thus, if the band-pass-filter employed has sufficiently narrow-band characteristics, the spectral component $X_i(k)$ of the narrow-band signal $x_i(n)$ with the discrete frequency band $[k_i - \Delta k, k_i + \Delta k]$ can be approximated by the complex value $|X(k_i)| \exp(\mathrm{j}\, 2\pi(k - k_0)\tau_0)$, that is,

$$X_i(k; m) \cong |X(k_i)|\, \mathrm{e}^{\mathrm{j}\, 2\pi(k-k_0)\tau_0}. \qquad (9)$$

Thus, the spectrum $X_i(k;m)$ of the mth block narrow-band signal $x_i(n;m) = x_i(n)*\delta(n-\tau_m)$ is approximately given by the constant values $X(k_i;m)$ of equation (9) multiplied by the term $\exp(-\mathrm{j}\,2\pi k\tau_m)$ due to the time delay from the mth ignition timing as

$$X_i(k;m) \cong |X(k_i)|\mathrm{e}^{\mathrm{j}\,2\pi(k-k_0)\tau_0} \times \mathrm{e}^{-\mathrm{j}\,2\pi k\tau_m} \tag{10}$$

$$= C_0|X(k_i)|\mathrm{e}^{\mathrm{j}\,2\pi k(\tau_0-\tau_m)}, \tag{11}$$

where $C_0 = \exp(-\mathrm{j}\,2\pi k_0\tau_0)$. By adding the noise term to the above equation,

$$Y_i(k;m) \cong C_0|X(k_i)|\mathrm{e}^{\mathrm{j}\,2\pi k(\tau_0-\tau_m)} + W_i(k;m) \quad (\text{for } k_i-\Delta k \le k \le k_i+\Delta k), \tag{12}$$

where $W_i(k;m)$ is the spectrum of the mth narrow-band signal $w_i(n;m)$ with the discrete frequency band $[k_i-\Delta k, k_i+\Delta k]$. Using this approximation, the spectrum $Z_i(k;m)$ of the squared signal $z_i(n;m)$ in equation (8) is approximately given by

$$\begin{aligned} Z_i(k;m) &= \frac{1}{N_0}\sum_{l=k_i-\Delta k}^{l=k_i+\Delta k}\Big\{X_i(l;m)X_i^*(l-k;m) \\ &\quad + X_i(l;m)W_i^*(l-k;m) \\ &\quad + W_i(l;m)X_i^*(l-k;m) \\ &\quad + W_i(l;m)W_i^*(l-k;m)\Big\} \\ &\cong \frac{1}{N_0}|C_0|^2|X(k_i)|^2\mathrm{e}^{\mathrm{j}\,2\pi k(\tau_0-\tau_m)}\Delta B_N \\ &\quad + \frac{1}{N_0}\sum_{l=k_i-\Delta k}^{l=k_i+\Delta k}\Big[C_0|X(k_i)| \\ &\quad \times W_i^*(l-k;m)\mathrm{e}^{\mathrm{j}\,2\pi l(\tau_0-\tau_m)} \\ &\quad + C_0^*|X(k_i)|W_i(l;m)\mathrm{e}^{-\mathrm{j}\,2\pi(l-k)(\tau_0-\tau_m)} \\ &\quad + W_i(l;m)W_i^*(l-k;m)\Big] \end{aligned} \tag{13}$$

where $\Delta B_N = 2\Delta k+1$ and $|C_0|^2 = 1$. Since the spectrum $W_i(k;m)$ of the narrow-band noise component $w_i(n;m)$ has random phase characteristics, the second and third terms are sufficiently smaller than the first term, and the fourth term is also sufficiently smaller than the first term if $k \neq 0$. Let us denote the sum of these three terms by $\Delta B_N \cdot Z_{iw}(k_i;m)$, then the spectrum $Z_i(k;m)$ in equation (13) is given by

$$Z_i(k;m) \cong \frac{\Delta B_N}{N_0}\Big[|X(k_i)|^2\mathrm{e}^{-\mathrm{j}\,2\pi k(\tau_0-\tau_m)} + Z_w(k_i;m)\Big] \quad (-2\Delta k \le k \le 2\Delta k, k \neq 0). \tag{14}$$

Though the effect on the phase characteristics due to the fluctuation in the lag values $\{\tau_m\}$ is large at the frequencies k around the resonant frequency k_0, the effect is small for frequencies around the d.c. component ($-2\Delta k \le k \le 2\Delta k$, $k \neq 0$). Thus the phase shift due to the fluctuation in the lag term τ_m is reduced by the squaring operation.

As is shown in equation (14), the spectrum $Z_i(k;m)$, ($i = a, b$) of the squared signal $z_i(n;m)$ consists of the following two components: one is the spectrum $Z_{ix}(k;m)$ of the band-limited damped sinusoidal signal $x_i(n;m)$ around the k_i-th frequency component, and the other is the spectrum $Z_{iw}(k;m)$ of the remaining components, including the band-limited noise $w_i(n;m)$ as follows:

$$Z_i(k;m) = \frac{\Delta B_N}{N_0}\{Z_{ix}(k;m) + Z_{iw}(k;m)\}, \tag{15}$$

where $i = a, b$, and

$$Z_{ix}(k;m) = |X(k_i)|^2\mathrm{e}^{-\mathrm{j}\,2\pi k(\tau_0-\tau_m)}. \tag{16}$$

By using the spectrum $Z_i(k;m)$ of the squared signal $z_i(n;m) = |y_i(n;m)|^2$, let us define the magnitude of the transfer function $H_{ab}(k)$ from the k_a-th frequency component to the k_b-th one as follows:

$$|H_{ab}(k)| = \left|\frac{E\big[Z_a^*(k;m)Z_b(k;m)\big]}{E\big[Z_a^*(k;m)Z_a(k;m)\big]}\right|. \tag{17}$$

By substituting equation (15) into equation (17), the cross spectrum between the two squared signals $z_a(n;m)$ and $z_b(n;m)$ in the numerator of equation (17) is given by

$$\begin{aligned} &E\big[Z_a^*(k;m)Z_b(k;m)\big] \\ &= \frac{\Delta B_N^2}{N_0^2}E\Big[\{Z_{ax}^*(k;m) + Z_{aw}^*(k;m)\} \\ &\qquad \times \{Z_{bx}(k;m) + Z_{bw}(k;m)\}\Big] \\ &= \frac{\Delta B_N^2}{N_0^2}\Big\{E\big[Z_{ax}^*(k;m)Z_{bx}(k;m)\big] \\ &\qquad + E\big[Z_{ax}^*(k;m)Z_{bw}(k;m)\big] \\ &\qquad + E\big[Z_{aw}^*(k;m)Z_{bx}(k;m)\big] \\ &\qquad + E\big[Z_{aw}^*(k;m)Z_{bw}(k;m)\big]\Big\}. \end{aligned} \tag{18}$$

During the averaging operation, the second and third terms of equation (18) approach zero since it can be assumed that the noise component $Z_{iw}(k;m)$ has no correlation with any other frequency components of the resonant vibration component $Z_{ix}(k;m)$. The fourth term also approaches zero except for the d.c. component (k=0). That is, the cross spectrum $E\big[Z_a^*(k;m)Z_b(k;m)\big]$ in equation (18) is approximately given by

$$E\big[Z_a^*(k;m)Z_b(k;m)\big] \cong \frac{\Delta B_N^2}{N_0^2}E\big[Z_{ax}^*(k;m)Z_{bx}(k;m)\big], \quad (k \neq 0) \tag{19}$$

if the number M of the averaging operation is sufficient large. Therefore, the noise component, which cannot be decreased in equation (7), is reduced by the averaging operation in equation (18).

In the same manner, the auto-spectrum component $|Z_a(k;m)|^2$ of $z_a(n;m)$ in the denominator of equation (17) is approximately given by

$$E\big[Z_a^*(k;m)Z_a(k;m)\big] \cong \frac{\Delta B_N^2}{N_0^2}\Big\{E\big[Z_{ax}^*(k;m)Z_{ax}(k;m)\big] + E\big[Z_{aw}^*(k;m)Z_{aw}(k;m)\big]\Big\} \quad (k \neq 0). \tag{20}$$

Thus, the magnitude of the transfer function in equation (17) is given by

$$|H_{ab}(k)| \cong \frac{\Big|E\big[Z_{ax}^*(k;m)Z_{bx}(k;m)\big]\Big|}{E\big[|Z_{ax}(k;m)|^2\big] + E\big[|Z_{aw}(k;m)|^2\big]}, \tag{21}$$

$(k \neq 0)$, when the number M of the averaging operation is sufficiently large. By substituting equation (16), the cross spectrum of the numerator of equation (21) is approximately given by

$$\Big|E\big[Z_{ax}^*(k;m)Z_{bx}(k;m)\big]\Big| \cong |X(k_a)|^2|X(k_b)|^2. \tag{22}$$

On the other hand, the auto-term in the denominator of equation (21) can be approximately described as follows: When the discrete frequency k_a almost coincides with the resonant frequency k_0 of the defect-induced vibration, the spectral component $Y_a(k;m)$ of $y_a(n;m)$ is dominant in the spectrum. If frequency k_a is near the resonant frequency k_0, it can be assumed that the SNR around the frequency k_a is very high and the spectral component $W_a(k;m)$ of the narrow-band noise $w_a(n;m)$ is negligibly small compared with the spectrum $X_a(k;m)$ of the defect-induced narrow-band signal $x_a(n;m)$. For this situation, the auto-power spectrum $|Z_a(k;m)|^2$ in the denominator of equation (19) is approximately represented by

$$\begin{aligned} E\big[|Z_a(k)|^2\big] &= \frac{\Delta B_N^2}{N_0^2}E\big[|Z_{ax}(k)|^2\big] + \frac{\Delta B_N^2}{N_0^2}E\big[|Z_{aw}(k)|^2\big] \\ &\cong \frac{\Delta B_N^2}{N_0^2}E\big[|Z_{ax}(k;m)|^2\big], \end{aligned} \tag{23}$$

if $k_a \cong k_0$. By substituting equation (16) into equation (23),

$$E\big[|Z_a(k)|^2\big] \cong \frac{\Delta B_N^2}{N_0^2}|X(k_a)|^4, \text{ if } k_a \cong k_0. \tag{24}$$

Substituting equations (22) and (24) into the numerator and the denominator of equations (17) or (21),

$$|H_{ab}(k)| \cong \frac{|X(k_a)|^2|X(k_b)|^2}{|X(k_a)|^4} = \frac{|X(k_b)|^2}{|X(k_a)|^2}. \tag{25}$$

From equation (25), the power spectrum estimate $|\widehat{X}(k_b)|^2$ for a frequency k_b is obtained as follows:

$$\begin{aligned} |\widehat{X}(k_b)|^2 &= |X(k_a)|^2|H_{ab}(k)| \\ &\cong E\big[|Y(k_a;m)|^2\big]\left|\frac{E\big[Z_a^*(k;m)Z_b(k;m)\big]}{E\big[Z_a^*(k;m)Z_a(k;m)\big]}\right| \\ &\qquad (k \neq 0, k_a \cong k_0). \end{aligned} \tag{26}$$

Thus, the magnitude of the power spectrum $|\widehat{X}(k_b)|^2$ is estimated by the product of the average magnitude of the dominant component, $E\big[|Y(k_a;m)|^2\big]$, in the power spectrum of $y(n)$ multiplied by the estimated magnitude $|H_{ab}(k)|$ of the transfer function $H_{ab}(k)$ from the k_a-th frequency component to the k_b-th frequency component as defined for the squared signals $z_a(n)$ and $z_b(n)$ in equation (17). By this estimation, the noise component due to the noise power in the second term of equation (7) is successfully decreased by the averaging operation even if the SNR is very low.

In this paper, it has been assumed that only one resonant vibration $x(n)$ is driven by the defect as shown in Figure 3(a-1). However, also in the case where more than one resonant vibration, $x_1(n)$ and $x_2(n)$, is driven simultaneously as shown in Figure 3(a-2), the transfer function $H_{ab}(k)$ from the k_a-th component of $x_1(n)$ to the k_b-th component of $x_2(n)$ can be estimated by the same procedure as is described above.

3. Simulation experiments

In the computer simulation experiments, white noise $w(n)$ is added to the almost periodic damped sinusoidal signal $x(n)$ in Figure 1(d). There are fluctuations in the lag terms $\{\tau_m\}$ in equation (2). The ratio of the standard deviations of the actual lag terms $\{\tau_m \times T_s\}$ to the inverse of the centre of the resonant frequency $f_0 = \omega_0/2\pi$ is 2, which is sufficiently large. For this condition, both components of the resonant vibration and noise in equation (6) decrease with the averaging operation.

Figures 4(a), (b), and (c) show the power spectral estimates $|\widehat{X}(k_b)|^2$ in equation (26) obtained by the proposed method for various SNR cases. The SNR are 0 dB, -5 dB, and -10 dB, respectively, the discrete band width $2\Delta k$ of each band-limited signal $y_i(n)$ is $\pm$ $0.01T_S$, where T_S is the sampling frequency, and the average number M is 500 in each case. The proposed method accurately estimates the power spectrum of the damped sinusoidal signal, which is closer to the true power spectrum $|X(k)|^2$ than the FFT-based power spectrum $P_y(k)$ estimated in equation (7).

Figures 5(a), (b), and (c) show the power spectra $|\widehat{X}(k_b)|^2$ estimated by the proposed method when the average numbers M are 500, 100, and 10, respectively. The SNR is -10 dB in these three cases. From these figures, by increasing the average number M, both the variance and the noise component are reduced according to $20\log_{10}(1/\sqrt{M})$ [dB].

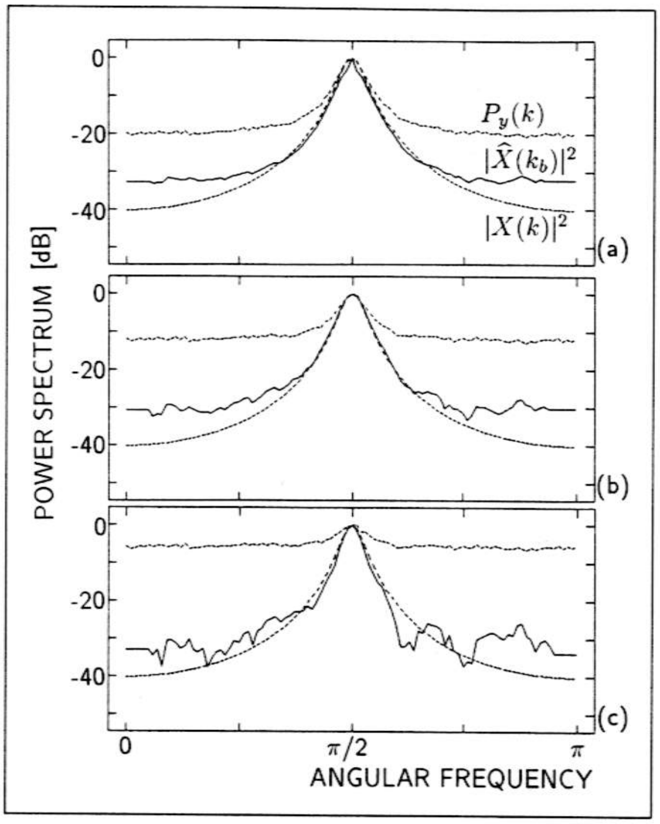

Figure 4. The estimated power spectra $|\widehat{X}(k)|^2$ of equation (26) for the aperiodic damped sinusoidal signal $x(n)$ in Figure 1(a) contaminated by high level white noise $w(n)$. The average number M is 500. Each block length N_0 is 512 points. (a)S/N=0 dB, (b)S/N=-5 dB, and (c)S/N=-10 dB
$|X(k)|^2$: The true power spectrum of $x(n)$.
$|\widehat{X}(k_b)|^2$: The power spectrum estimated from $y(n)$ by the proposed method in equation (26).
$P_y(k)$: The power spectrum estimated from $y(n)$ by the standard FFT-based method in equation (7).

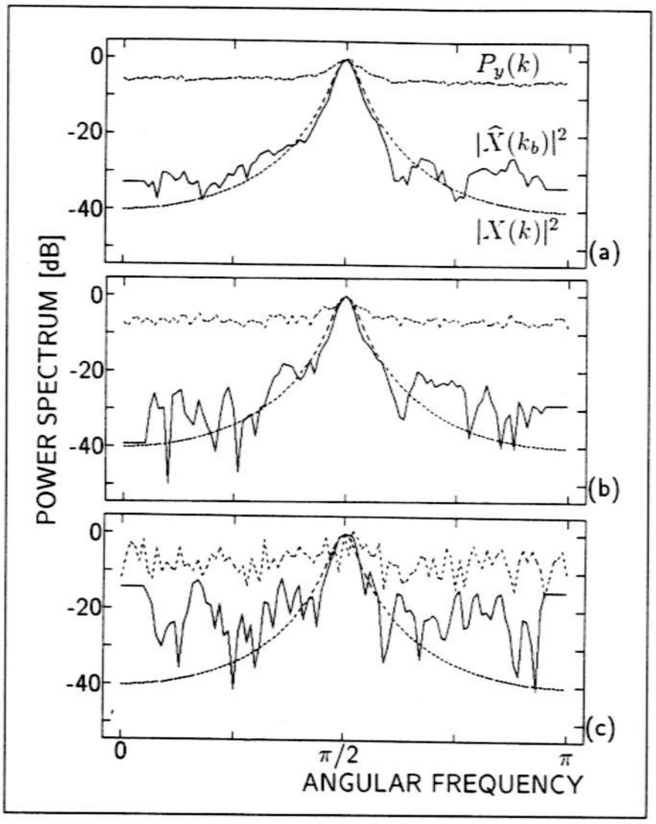

Figure 5. The estimated power spectra $|\widehat{X}(k)|^2$ of equation (26) for the aperiodic damped sinusoidal signal $x(n)$ in Figure 1(a) contaminated by high-level white noise $w(n)$. The SNR is -10 dB. Each block length N_0 is 512 points. The average number M is (a)500, (b)100 and (c)10.
$|X(k)|^2$: The true power spectrum of $x(n)$.
$|\widehat{X}(k_b)|^2$: The power spectrum estimated from $y(n)$ by the method proposed in equation (26).
$P_y(k)$: The power spectrum estimated from $y(n)$ by the standard FFT-based method in equation (7).

4. Application Experiments

In the computer simulation experiments, the dominant frequency component was given *a priori*. However, for actual automobile systems, the dominant frequency components are unknown. Thus, it is necessary to determine the discrete resonant frequency k_0 of the defect-induced signal.

To begin with, using the spectra $\{Z_i(k;m)\}$ of the squared signals $\{z_i(n;m)\}$, let us calculate the following squared coherence function $|\gamma_{ab}(k)|^2$ between the k_a-th frequency component and the k_b-th frequency component:

$$|\gamma_{ab}(k)|^2 = \frac{|E[Z_a^*(k;m)Z_b(k;m)]|^2}{E[|Z_a(k;m)|^2]E[|Z_b(k;m)|^2]}. \quad (27)$$

This equation corresponds to the squared coherence function of the transfer function defined in equation (21). The squared coherence function $|\gamma_{ab}(k)|^2$ between each pair of two different frequency components is shown in Figures 6(a) and 6(b) for a normal sample and for a defective sample, respectively, in order to determine the frequency band of the defect-induced signal $x(n)$. Figure 6(a) shows that there is a correlation only for the cases where two frequencies are identical, that is, $k_a = k_b$. For the results of the defect sample in Figure 6(b), however, there is a correlation between the components from 2 kHz to 6 kHz. Thus, 4 kHz was chosen as the discrete centre frequency k_a/N_0T_S of the resonant vibration in the following experiments.

Next, the transfer function $H_{ab}(k)$ of equation (17) from the squared narrow-band component around k_a/N_0T_S=4 kHz to other components with k_b/N_0T_S is calculated to estimate the power spectrum $|\widehat{X}(k_b)|^2$ in equation (26) of the defect-induced signal $x(n)$, where each block length N_0 is 512 points and $T_S = 20\,\mu s$. Figures 7(a) and 7(b) show the power spectral estimates $|\widehat{X}(k_b)|^2$ obtained by the proposed method in equation (26) and the power spectral estimates $P_y(k)$ in the standard method of equation (17), for the signals radiated from a normal engine and from a defective engine, when the average number M is 100. Each figure also shows the squared coherence function $|\gamma_{ab}(k)|^2$ in equation (27) for k_a/N_0T_S=4 kHz. For the $|\gamma_{ab}(k)|^2$ of the normal sample in Figure 7(a), all the frequency components except k_a are reduced by the averaging operation since they do not have a correlation with the k_a component. For the defective sample in Figure 7(b), however, the frequency components

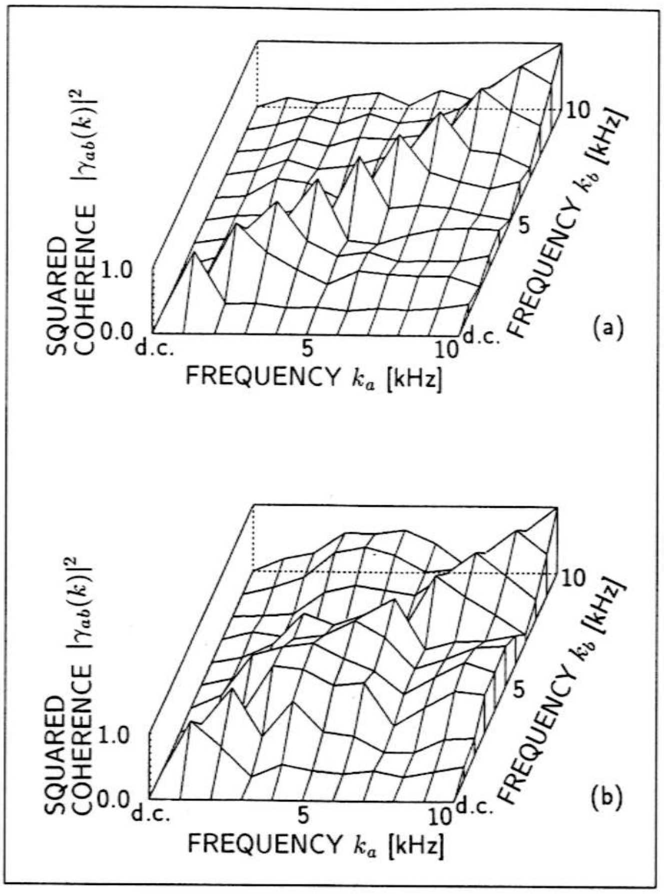

Figure 6. The squared coherence function $|\gamma_{ab}(k)|^2$ between each pair of different frequency components calculated from the squared narrow-band signal of the observed signal $y(n)$ radiated from an automobile engine.
(a) The squared coherence function $|\gamma_{ab}(k)|^2$ for a normal sample.
(b) The squared coherence function $|\gamma_{ab}(k)|^2$ for a sample with defective gears.

of $|\gamma_{ab}(k)|^2$ from 2 kHz to 6 kHz remain through the averaging operation. Thus, they are correlated with the 4 kHz component.

From the *simulation* experiments, the spectrum of the resonant vibration, which has wide-band characteristics and correlates with different frequency bands around the resonant frequency, is successfully estimated even in low SNR cases. Though the *actual* spectra cannot be measured in the application experiments, the power spectrum $|\widehat{X}(k_b)|^2$ of the defect-induced vibration is estimated as shown in Figure 7.

5. Conclusions

In this paper, we have proposed a method to estimate accurately the power spectrum of a damped sinusoidal signal in low SNR cases by calculating the transfer function between two different frequency components of the observed signal.

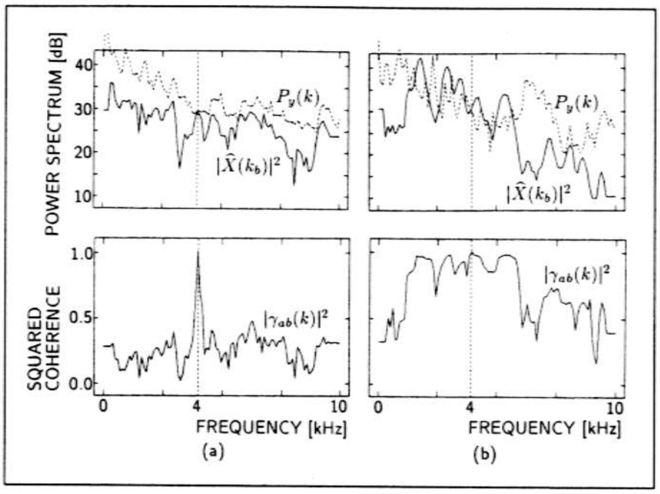

Figure 7. The estimated power spectrum for the defect-induced signal. Each block length N_0 is 512 points.
$|\widehat{X}(k_b)|^2$: The power spectrum estimated from $y(n)$ by the method proposed in equation (26).
$P_y(k)$: The power spectrum estimated from $y(n)$ by the standard FFT-based method in equation (7).
(a) for the normal sample in Figure 6.
(b) for the sample with defective gears in Figure 6.

From the computer simulations, the principle of the proposed method was confirmed. The noise components were reduced by applying an averaging operation to the cross spectrum between the squared narrow-band signals. By applying the proposed method to an actual automobile system, the frequency band of the defect-induced signal was first identified by the squared coherence function. Using the resultant resonant frequency, the power spectrum of the defect-induced signal was estimated by the proposed method.

Acknowledgement

We would like to thank Dr. Hideo Suzuki of Ono Sokki Co. Ltd. for his valuable discussion and suggestions.

References

Imai, M., Kanai, H., Chubachi, N., Oguro, S., and Suzuki, H. (June 1993). A new method for quantitative measurement of correlation defined between different frequency band components. *The Journal of the Acoustical Society, Japan* **49(6)**, 389–396. (in Japanese).
Kanai, H., Abe, M., and Kido, K. (1986). Detection and discrimination of flaws in ball bearings by vibration analysis. *The Journal of the Acoustical Society, Japan* **E-9(2)**, 121–132.
Oppenheim, A. V. and Schafer, R. W. (1975). *Digital Signal Processing*. Prentice-Hall Inc., Englewood Cliffs, NJ, USA.
Welch, P. D. (June 1967). The use of fast Fourier transform for the estimation of power spectrum: A method based on time averaging over short, modified periodgrams. *IEEE Transactions on Audio and Electroacoustics* **AU-15(2)**, 70–73.